Environ. Sci. Technol. **2007**, *41,* 6541−6546

Electrochemical Oxidation Characteristics of p-Substituted Phenols Using a Boron-Doped Diamond Electrode

XIUPING ZHU,[†] SHAOYUAN SHI,[‡] JUNJUN WEI,[§] FANXIU LV,[§] HUAZHANG ZHAO,[†] JIANGTAO KONG,[†] QI HE,[§] AND JINREN NI*,[†]

College of Environmental Science and Engineering, Peking University, The Key Laboratory of Water and Sediment Sciences, Ministry of Education, Beijing 100871, China, National Key Laboratory of Biochemical Engineering, Institute of Process Engineering, Chinese Academy of Sciences, Beijing 100080, China, and Department of Material Science and Engineering, University of Science and Technology Beijing, Beijing 100083, China

Electrochemical oxidation of some p-substituted phenols (*p*-nitrophenol, *p*-hydroxybenzaldehyde, phenol, *p*-cresol, and *p*-methoxyphenol) with electron-donating and -withdrawing substituents was studied to reveal the relationship between the structure and the electrochemical reactivity of p-substituted phenols using a boron-doped diamond electrode by voltammetry and bulk electrolysis. Voltammetric study shows that the oxidation peak potentials of p-substituted phenols become more positive with an increase of Hammett's constants, that is, the direct electrochemical oxidation of p-substituted phenol with an electron-withdrawing group is more difficult than that of p-substituted phenol with an electron-donating group. However, the p-substituted phenols with electron-withdrawing groups are degraded faster than those with electron-donating groups in bulk electrolysis, which is opposite to the result obtained on the Pt electrode. These results indicate that the p-substituted phenols are mainly degraded by indirect electrochemical oxidation with hydroxyl radicals on a boron-doped diamond electrode. Under the attack of hydroxyl radicals, the release of p-substituted groups from the aromatic ring is the rate-limiting step. Since electron-withdrawing groups are easy to be released, the p-substituted phenols with these groups are degraded faster than those with electron-donating groups. Therefore, the degradation rates of the p-substituted phenols rise with an increase of Hammett's constants.

Introduction

Phenols are common pollutants in effluents from coking, oil refineries, production of pesticides and herbicides, dyes and textiles, pharmaceuticals, pulp and paper, plastics, and detergent, etc. Because most of these compounds are toxic or non-biodegradable, conventional biological methods are not suitable for their removal.

Advanced oxidation processes (AOPs), including Fenton oxidation, ozonation, wet air oxidation, photocatalytic oxidation, supercritical water oxidation, and electrochemical oxidation, were studied for the treatment of the wastewater containing phenols. Among them, electrochemical oxidation is one of the most promising technologies that is environmental friendly and can oxidize toxic organic compounds effectively (*1*).

Electrode material is crucial for optimizing electrochemical oxidation processes. In the past three decades, many electrode materials have been tested to improve the current efficiency and reduce the cost, including graphite, platinum (*2*), IrO_2 (*3*), SnO_2 (*4*), PbO_2 (*5*), and boron-doped diamond (BDD) (*6*). The BDD electrode is distinguished from conventional electrodes because of several important technological properties, such as an extremely wide potential window, corrosion stability in very aggressive media, an inert surface with low adsorption properties, a strong tendency to resist deactivation, and robust oxidation capacity (*6*). Recently, the BDD electrode has attracted more and more attention in wastewater treatment processes.

It has been proven that BDD electrodes were very effective in removing various biorefractory organic pollutants, including phenol (*7*, *8*), polyhydroxybenzenes (*9*), chlorophenols (*10*−*13*), nitrophenols (*14*−*16*), benzoic acid (*17*), aniline (*18*), 2-naphthol (*19*), surfactants (*20*), dyes (*21*), herbicides (*22*), 3-methylpyridine (*23*), triazines (*24*), and polyacrylates (*25*). Depending on different applied potentials, the oxidation of organics at BDD electrodes can be divided into two mechanisms: direct electrochemical oxidation in the potential region before oxygen evolution (water stability) and indirect electrochemical oxidation via electrogenerated hydroxyl radicals in the potential region of oxygen evolution (water decomposition).

However, very few studies examined the relationship between the structure of organic compounds and their electrochemical activity. Nasr et al. investigated the electrochemical oxidation of hydroquinone, resorcinol, and catechol on BDD anodes (*26*). Their study indicated that although no differences existed in the bulk electrolysis process, different voltammetric behavior between resorcinol and the other two isomers was observed. Studies on electrochemical oxidation of *p*-nitrophenol, *p*-hydroxybenzoic acid, hydroquinone, *p*-chlorophenol, phenol, and *p*-aminophenol on Pt electrodes revealed that compounds with electron-donating substituents were easier to remove and that their initial degradation rates were correlated to the octanol−water partitioning coefficient (log P_{oct}) and Hammett's constant (*2*). Unfortunately, a similar report on BDD electrodes has not been found so far. It is well-known that the anode material is crucial in the specific interaction between the anode surface and the compounds. At the surfaces of SnO_2, PbO_2, and BDD, H_2O is discharged to produce physisorbed active oxygen (adsorbed hydroxyl radicals), and organic compounds mainly undergo electrochemical combustion, which can completely oxide compounds to CO_2 and H_2O. Whereas at the surfaces of IrO_2, Pt, and RuO_2, H_2O is discharged to form chemisorbed active oxygen (oxygen in the oxide lattice), and organic pollutants mainly undergo electrochemical conversion to highly oxidized products after a series of electrochemical and chemical steps (*2*, *27*).

This paper investigates the electrochemical oxidation of p-substituted phenols with different electron-donating and

* Corresponding author phone: +86 10 6275 1185; fax: +86 10 6275 6526; e-mail: nijinren@iee.pku.edu.cn.
[†] Peking University.
[‡] Chinese Academy of Sciences.
[§] University of Science and Technology Beijing.

10.1021/es070955i CCC: $37.00
Published on Web 08/10/2007

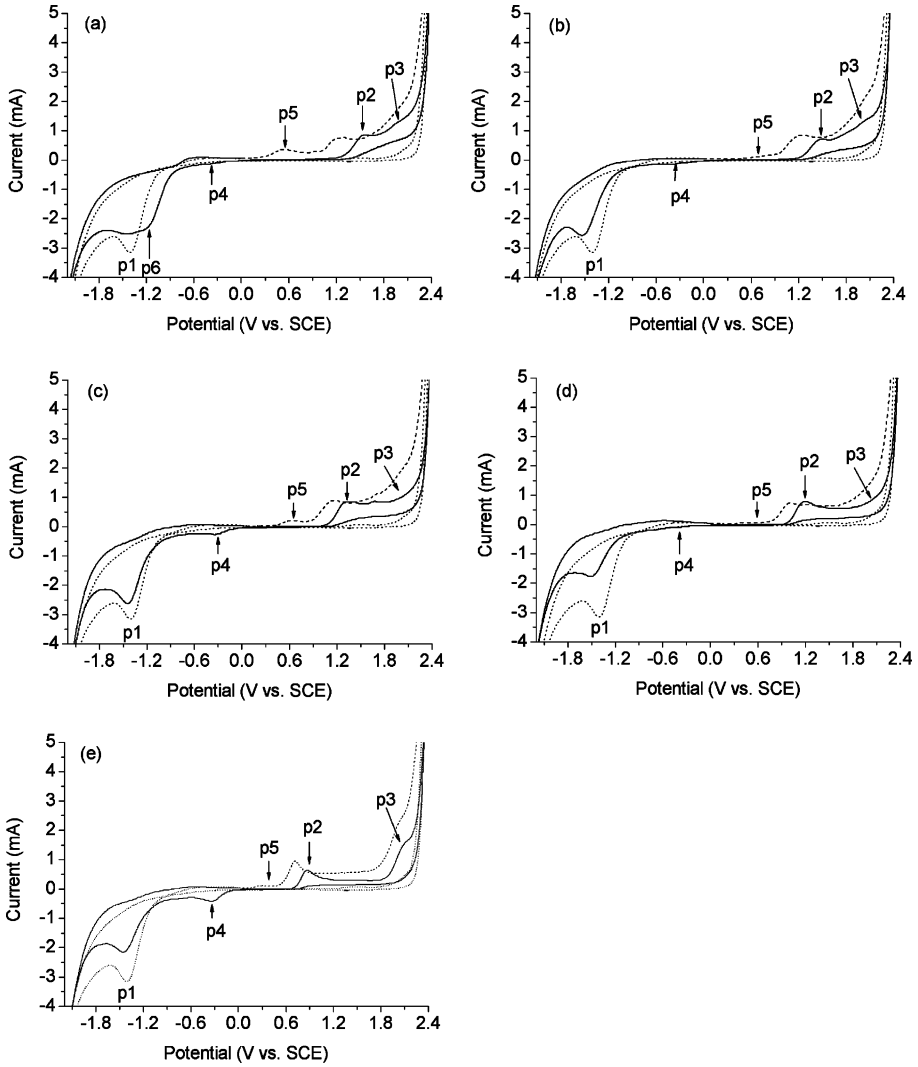

FIGURE 1. Cyclic voltammograms on BDD electrode of 1 mM *p*-nitrophenol (a), *p*-hydroxybenzaldehyde (b), phenol (c), *p*-cresol (d), and *p*-methoxyphenol (e) in 0.2 M Na_2SO_4 media at pH 12. Scan rate: 100 mV s^{-1}. Auxiliary electrode: Pt. Reference electrode: SCE. Dotted line: blank; solid line: first cycle; and dashed line: second cycle.

-withdrawing substituents, and particular attention was paid to the effect of the electronic nature of substituents on the electrochemical reactivity of compounds using a BDD electrode.

Experimental Procedures

Electrochemical Measurements. The electrochemical measurements were performed with a CHI 760B electrochemical workstation (Shanghai Chenhua) in a conventional three-electrode cell at room temperature (20 °C). The working volume of the cell was 60 mL. A BDD electrode with an exposed geometric area of 4 cm^2 was used as the working electrode. The BDD electrode was prepared using a microwave plasma-assisted CVD system with an output frequency of 2.45 GHz. The Ti substrates were first scrubbed by 200 and 800 grid sandpapers, then polished with 1.5 μm diamond paste, and finally cleaned by acetone and alcohol. The reactant gas was a mixture of H_2, CH_4, and B_2H_6. The flow rates of H_2 and CH_4 were 198 and 2 sccm, respectively. The ratio of B/C was 5000 ppm. A platinum plate was used as the counter electrode, while a saturated calomel electrode (SCE) was used as the reference electrode in a separate compartment with a Luggin capillary (all potentials are quoted against SCE). Solutions were prepared using Milli-Q water (Millipore). The 0.2 M Na_2SO_4 was used as the supporting electrolyte. The pH of solution was adjusted to 12 using 1 M NaOH. Before each electrochemical measurement, the BDD electrode was anodically polarized at a fixed potential of 2.8 V for 20 s to reactivate the electrode surface.

Bulk Electrolysis. Bulk oxidation of p-substituted phenols was performed in a one-compartment cell under galvanostatic conditions (current density 20 mA cm^{-2}) at room temperature. The 250 mL solution was stirred by a magnetic stirring bar in the electrolysis process. A BDD electrode was used as an anode with a working geometric area of 4 cm^2. A copper sheet of the same size was used as the cathode. The electrode gap was set to 10 mm. The solution consisted of 1 mM p-substituted phenol and 0.2 M Na_2SO_4 with a pH of 12. Samples were collected from the cell at various intervals for chemical analysis.

Analytical Methods. The concentrations of *p*-nitrophenol, *p*-hydroxybenzaldehyde, phenol, *p*-cresol, and *p*-methoxyphenol were measured by using Agilent HP1100 HPLC with a ZORBAX SB-C^{18} column and a DAD detector. The mobile phase was methanol/water (50:50), and the flow rate was 1.0 mL min^{-1}. The UV detector was set at 314 nm for *p*-nitrophenol and 270 nm for other p-substituted phenols. COD was measured by a titrimetric method using dichromate as the oxidant in acidic solution at 150 °C for 2 h (Hachi). UV−vis spectra were obtained via Specord 200 (Analytikjena).

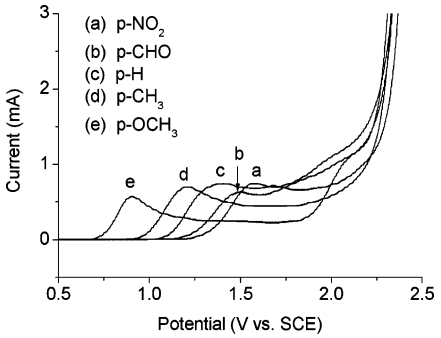

FIGURE 2. Linear sweep voltammograms on BDD anode of 1 mM *p*-nitrophenol (a), *p*-hydroxybenzaldehyde (b), phenol (c), *p*-cresol (d), and *p*-methoxyphenol (e) in 0.2 M Na_2SO_4 media at pH 12. Scan rate: 50 mV s^{-1}. Auxiliary electrode: Pt. Reference electrode: SCE.

Results and Discussion

Voltammetric Study. The cyclic voltammograms for *p*-nitrophenol (panel a), *p*-hydroxybenzaldehyde (panel b), phenol (panel c), *p*-cresol (panel d), and *p*-methoxyphenol (panel e) on a BDD electrode at a scan rate of 100 mV s^{-1} are presented in Figure 1. The blank curve (0.2 M Na_2SO_4, pH 12 adjusted by NaOH) obtained under the same experimental conditions is shown for comparison (Figure 1, dotted lines). A cathodic current peak (p1) occurred at about −1.4 V possibly because of the reduction of peroxodisulfate ($S_2O_8^{2-}$), which was formed by the oxidation of sulfate (SO_4^{2-}) at a high potential (*9*, *14*). For all p-substituted phenols, two anodic current peaks (p2 and p3) and a new cathodic current peak (p4) occurred in the first scan (Figure 1, solid lines). The cathodic current peak (p1) was also observed for all phenols, but the peak current was lower relative to that of blank, which may have resulted from electrode fouling (*8*, *10*). In the second scan (Figure 1, dashed lines), a new anodic current peak (p5) appeared. Furthermore, the peaks of p2 and p3 shifted to be more negative. This shift could be attributed to the different surface properties of the BDD electrode. Right before each electrochemical measurement, the BDD electrode was anodically polarized at a fixed potential of 2.8 V for 20 s to reactivate the electrode surface, which could make the electrode surface oxygen-terminated. However, the electrode surface could become hydrogen-terminated in the second scan after scanning during the negative potential range. For *p*-nitrophenol, a special cathodic current peak (p6) was observed, which represented the reduction of *p*-nitrophenol to *p*-aminophenol (*14*).

Both peaks (p2 and p3) corresponded to the oxidation of p-substituted phenolate, the dominant species of all the p-substituted phenols at pH 12, to the p-substituted phenoxy radical and its subsequent oxidation to the p-substituted phenoxy cation (*10*, *12*, *14*) (eq 1). The X in the equations represents the substituents (-NO_2, -CHO, -H, -CH_3, and -OCH_3).

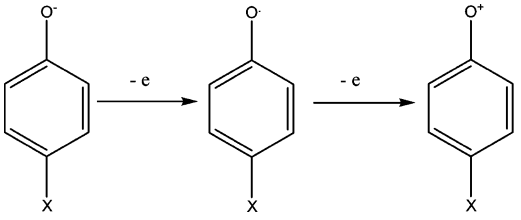

(1)

However, for different p-substituted phenols, the oxidation overpotentials depended on the p-substituted groups. Figure 2 shows the linear sweep voltammograms for p-substituted phenols on the BDD electrode at a scan rate of 50 mV s^{-1}. The oxidation peak potentials p2 of p-substituted

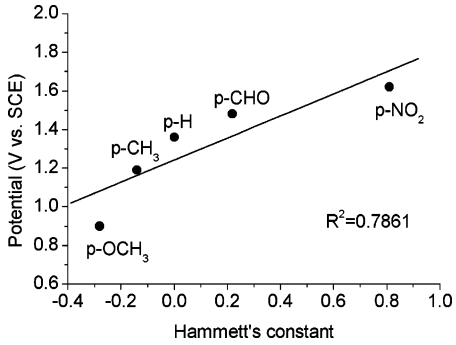

FIGURE 3. Relationship between oxidation peak potential p2 of p-substituted phenols and Hammett's constant.

phenols were +1.62 V for *p*-nitrophenol, +1.48 V for *p*-dihydroxybenzaldehyde, +1.36 V for phenol, +1.19 V for *p*-cresol, and +0.90 V for *p*-methoxyphenol, respectively. The peak potentials were correlated to Hammett's constants of the p-substituted phenols ($R^2 = 0.7861$), as shown in Figure 3. Hammett's constant represents the effect of different substituents on the electronic character of a given aromatic system. A positive value of Hammett's constant indicates an electron-withdrawing group, while a negative value indicates an electron-donating group. The oxidation peak potentials of p-substituted phenols became more positive with an increase of Hammett's constants (Figure 3). Hence, it can be concluded that the direct oxidation of p-substituted phenol with a poor electronic environment from an electron-withdrawing group was more difficult than that of p-substituted phenol with a rich electronic environment from an electron-donating group.

The two electrochemically formed compounds (p-substituted phenoxy radical and p-substituted phenoxy cation) were very reactive and could couple to form polymers or underwent other chemical transformations such as the addition of hydroxyl groups and the release of substituents (*12*) (eq 2).

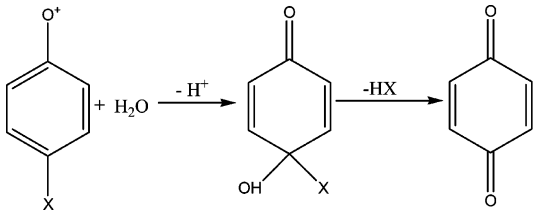

(2)

In the oxygen evolution region, indirect oxidation of p-substituted phenols might occur with hydroxyl radicals produced by water discharge (*8*, *19*). Both peaks (p4 and p5) corresponded to the reduction and oxidation of the benzoquinone/hydroquinone couple (*12*, *14*), as shown in eq 3, which confirmed the release of the substituents.

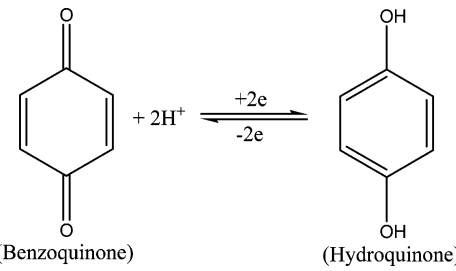

(3)

Bulk Electrolysis. The concentrations of the treated p-substituted phenols and COD were measured during electrolysis. Figure 4a shows the p-substituted phenol substrate concentration evolution as a function of electrical

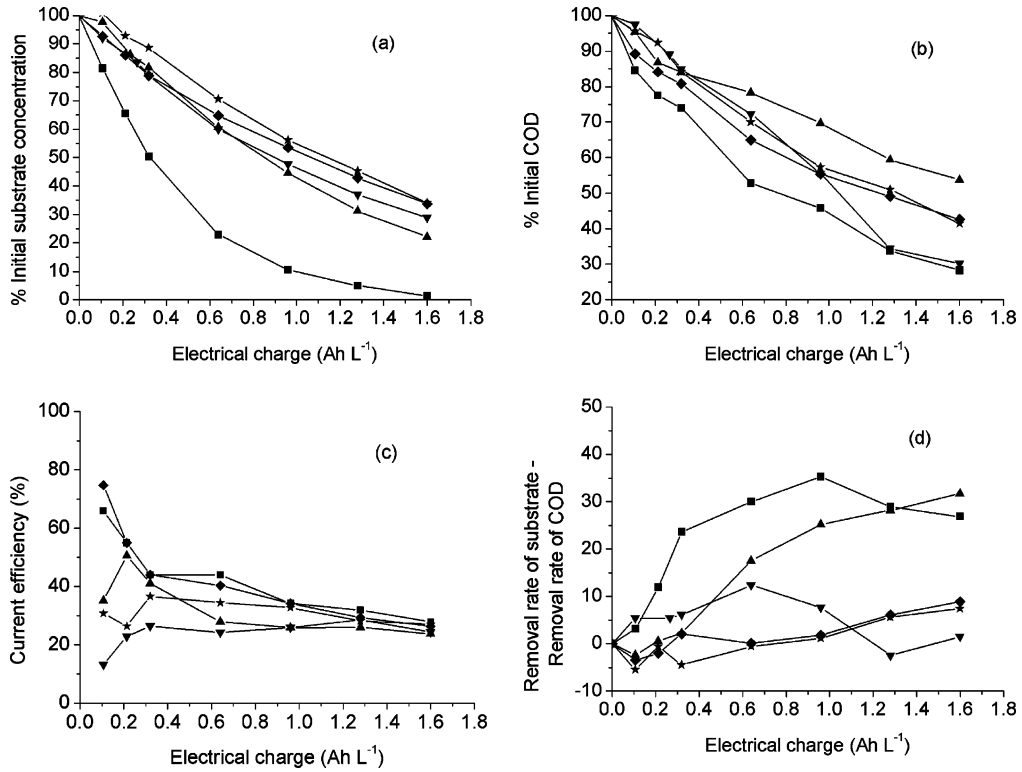

FIGURE 4. Electrochemical oxidation of p-substituted phenols as a function of electrical charge. Initial solution contains 1 mM substrate + 0.2 M Na_2SO_4 at pH 12. Substrate concentration (a), COD (b), current efficiency (c), and intermediates (d). Symbols: ■: *p*-nitrophenol, ▲: *p*-dydroxybenzaldehyde, ▼: phenol, ◆: *p*-cresol, and ★: p-methoxyphenol.

charge applied to the electrolytic cell. By the end of treatment (1.6 A h L^{-1}), the removal percentages of *p*-nitrophenol, *p*-hydroxybenzaldehyde, phenol, *p*-cresol, and *p*-methoxyphenol were 99, 78, 71, 67, and 66%, respectively. Figure 4b shows the COD evolution as a function of electrical charge. After 1.6 A h L^{-1} of electrolysis, the COD concentration in the *p*-nitrophenol, *p*-hydroxybenzaldehyde, phenol, *p*-cresol, and *p*-methoxyphenol systems decreased by 72, 46, 70, 57, and 58%, respectively. On the basis of the measured COD, the current efficiency (CE) was calculated using the following equation:

$$\mathrm{CE} = \frac{[\mathrm{COD}_t - \mathrm{COD}_{t+\Delta t}]FV}{8I\Delta t} \quad (4)$$

where COD_t and $\mathrm{COD}_{t+\Delta t}$ are the COD (in g of O_2 m^{-3}) at times t and $t + \Delta t$ (in s), respectively, F is Faraday's constant (96 487 C mol^{-1}), V is the volume of the electrolyte (in dm^3), I is the current (in A), and 8 is a dimensional factor for unit consistency (32 g of O_2 mol^{-1} of O_2/4 mol of e^{-1} mol^{-1} of O_2). Figure 4c shows the current efficiency changes with the applied electrical charge. The current efficiency of p-substituted phenol oxidation was about 20 to 50%.

The substrate removal rate was greater than the COD removal rate for each p-substituted phenol system, which indicated that part of the substrate was degraded to soluble intermediates (*8*, *10*, *14*) rather than completely oxidized to CO_2 and H_2O. In the electrolysis of phenols, the first step was the release of the p-substituted groups from the aromatic ring to form phenol or quinones. These organic compounds were oxidized first to carboxylic acids (maleic and oxalic acids) and then to carbon dioxide (*14*, *28*). Figure 4d shows the removal rate difference between substrate and COD as a function of electrical charge, which reflects the intermediate evolution with a change of applied electrical charge. It can be seen that the p-substituted phenols with electron-withdrawing groups (*p*-nitrophenol and *p*-hydroxybenzaldehyde) produced more intermediates than those with electron-donating groups (phenol, *p*-cresol, and *p*-methoxyphenol) in the electrolysis process.

Figure 5 shows the UV−vis absorption spectra of *p*-nitrophenol (panel a), *p*-hydroxybenzaldehyde (panel b), phenol (panel c), *p*-cresol (panel d), and *p*-methoxyphenol (panel e) electrolytes. Two new absorbance peaks appeared at 250 and 350 nm for *p*-nitrophenol after 3 h of electrolysis, which might represent the production of two intermediates, phenol and benzoquinone (*14*). For *p*-hydroxybenzaldehyde, two new absorbance peaks appeared at 220 and 280 nm after 2 h of electrolysis, which might indicate the generation of two intermediates, hydroquinone and benzoquinone (*28*). However, no new absorbance peaks were observed for other p-substituted phenols, which may be due to the slow release of p-substituted groups from these compounds and little accumulation of intermediates. Moreover, the yellow solution of *p*-nitrophenol changed to brown after electrolysis for 40 min, while the white solution of *p*-hydroxybenzaldehyde changed to light pink after electrolysis for 1 h. The change of color might be due to the accumulated intermediates, such as hydroquinone and benzoquinone.

To establish the relationship between the structure and the electrochemical reactivity, the degradation rate of the p-substituted phenols relative to that of phenol (r_{relative}) was plotted against Hammett's constant (Figure 6). The value of r_{relative} was calculated using the following equation:

$$r_{\mathrm{relative}} = \frac{\text{removal percentage of p-substituted phenol}}{\text{removal percentage of phenol}} \quad (5)$$
$$\text{(at 1.6 A h L}^{-1}\text{ electrolysis time)}$$

An apparent correlation between r_{relative} and Hammett's constant was obtained ($R^2 = 0.9828$). However, the degradation rates of p-substituted phenols rose with an increase of Hammett's constants, which was opposite of the result of the electrochemical degradation of p-substituted phenols on the

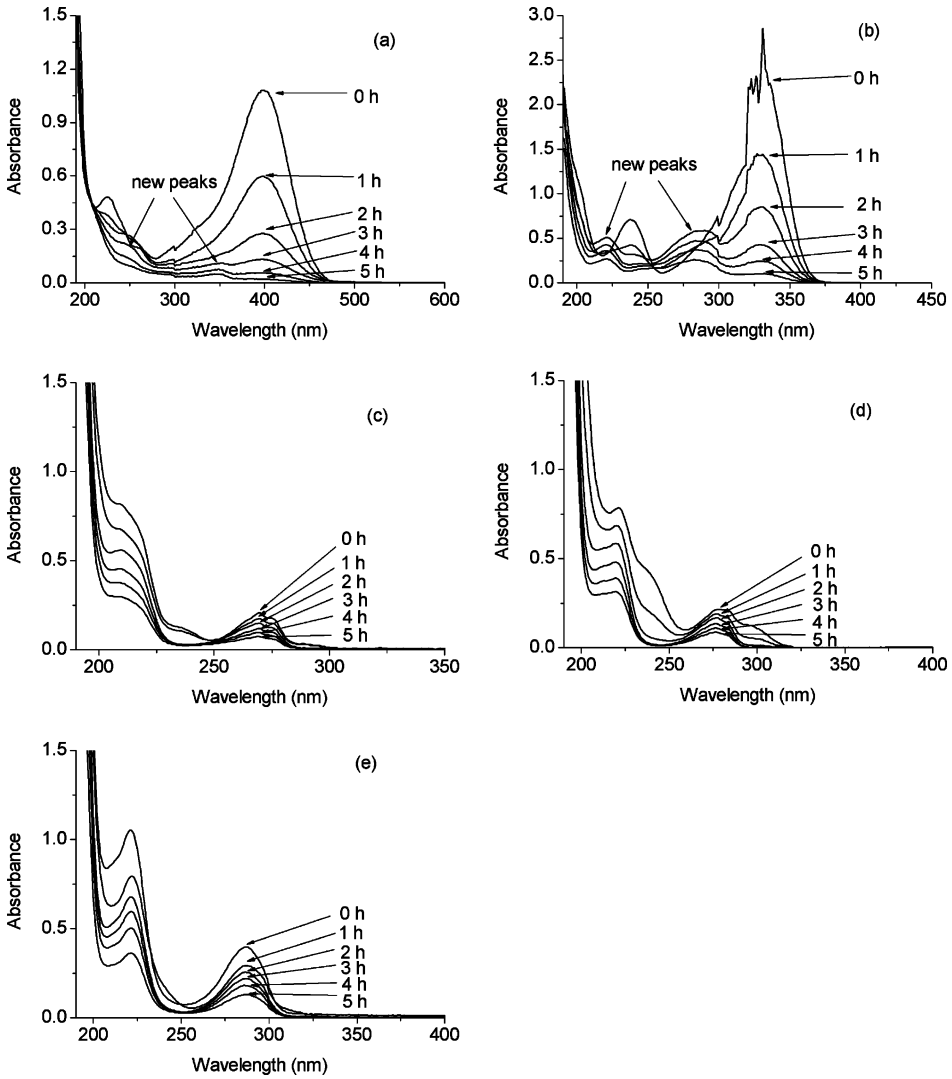

FIGURE 5. UV−vis absorption spectra of p-substituted phenol electrolytes. Initial solution contains 1 mM substrate + 0.2 M Na_2SO_4 at pH 12. *p*-Nitrophenol (diluted 10×) (a), *p*-dydroxybenzaldehyde (diluted 5×) (b), phenol (diluted 5×) (c), *p*-cresol (diluted 5×) (d), and *p*-methoxyphenol (diluted 5×) (e).

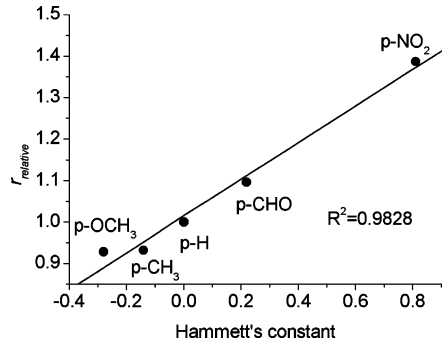

FIGURE 6. Relationship between $r_{relative}$ and Hammett's constant of p-substituted phenols.

Pt electrode (*2*). From the UV−vis absorption spectra of p-substituted phenols (Figure 5), it can be also seen that characteristic absorption peaks of *p*-nitrophenol (400 nm) and *p*-hydroxybenzaldehyde (325 nm) decreased faster than those of phenol (265 nm), *p*-cresol (280 nm), and *p*-methoxyphenol (290 nm). The difference may have resulted from the different properties of the Pt and BDD electrodes.

According to the generalized scheme of the electrochemical degradation of organic compounds on metal oxide anodes proposed by Comninellis (*27*), in the first stage, H_2O is discharged at the anode surface to produce adsorbed hydroxyl radicals (eq 6)

$$H_2O \rightarrow {}^{\bullet}OH + H^+ + e^- \quad (6)$$

For the Pt anode, which is active, the adsorbed hydroxyl radicals may interact with Pt to form PtO_X (eq 7)

$$Pt({}^{\bullet}OH) \rightarrow PtO_X + H^+ + e^- \quad (7)$$

In the presence of organics, the chemisorbed active oxygen (PtO_X) participates in the formation of selective oxidation products. One would expect facile electron transfer between the anode surface and the electron-rich compounds with electron-donating groups. Hence, the degradation rates of p-substituted phenols on the Pt anode increase with a decrease of Hammett's constants (*2*).

For the BDD electrode, which is inert and weak in adsorption (*6*), the physisorbed hydroxyl radicals produced from H_2O discharge may transfer to the vicinity of the anode and directly attack the substrates. In bulk electrolysis, p-substituted phenols were mainly degraded by indirect electrochemical oxidation with hydroxyl radicals. Under the attack of hydroxyl radicals, the removal of p-substituted groups from the aromatic ring was the rate-limiting step.

The detection of intermediates (hydroquinone, benzoquinone, phenol, and non-substituted carboxylic acids) in our experiments and in other papers (*14*, *28*) confirmed the release of p-substituted groups. Since electron-withdrawing groups are easily released, p-substituted phenols with these groups were degraded faster than p-substituted phenols with electron-donating groups. Hence, the degradation rates of the p-substituted phenols rose with an increase of Hammett's constants.

Acknowledgments

This work was supported by the National Basic Research Program of China under grant No. 2006BAB04A14. The authors acknowledge three anonymous reviewers for their very positive and helpful comments.

Literature Cited

(1) Jüttner, K.; Galla, U.; Schmieder, H. Electrochemical approaches to environmental problems in the process industry. *Electrochim. Acta* **2000**, *45*, 2575−2594.
(2) Torres, R.; Torres, W.; Peringer, P.; Pulgarin, C. Electrochemical degradation of p-substituted phenols of industrial interest on Pt electrodes. Attempt of a structure−reactivity relationship assessment. *Chemosphere* **2003**, *50*, 97−104.
(3) Fóti, G.; Gandini, D.; Comninellis, C.; Perret, A.; Haenni, W. Oxidation of organics by intermediates of water discharge on IrO_2 and synthetic diamond anodes. *Electrochem. Solid-State Lett.* **1999**, *2*, 228−230.
(4) He, D.; Mho, S. Electrocatalytic reactions of phenolic compounds at ferric ion co-doped SnO_2:Sb^{5+} electrodes. *J. Electroanal. Chem.* **2004**, *568*, 19−27.
(5) Zhou, M.; Dai, Q.; Lei, L.; Ma, C.; Wang, D. Long life modified lead dioxide anode for organic wastewater treatment: Electrochemical characteristics and degradation mechanism. *Environ. Sci. Technol.* **2005**, *39*, 363−370.
(6) Panizza, M.; Cerisola, G. Application of diamond electrodes to electrochemical processes. *Electrochim. Acta* **2005**, *51*, 191−199.
(7) Hagans, P. L.; Natishan, P. M.; Stoner, B. R.; O'Grady, W. E. Electrochemical oxidation of phenol using boron-doped diamond electrodes. *J. Electrochem. Soc.* **2001**, *148*, 298−301.
(8) Iniesta, J.; Michaud, P. A.; Panizza, M.; Cerisola, G.; Aldaz, A.; Comninellis, C. Electrochemical oxidation of phenol at boron-doped diamond electrode. *Electrochim. Acta* **2001**, *46*, 3573−3578.
(9) Cañizares, P.; Sáez, C.; Lobato, J.; Rodrigo, M. A. Electrochemical oxidation of polyhydroxybenzenes on boron-doped diamond anodes. *Ind. Eng. Chem. Res.* **2004**, *43*, 6629−6637.
(10) Rodrigo, M. A.; Michaud, P. A.; Duo, I.; Panizza, M.; Cerisola, G.; Comninellis, C. Oxidation of 4-chlorophenol at boron-doped diamond electrode for wastewater treatment. *J. Electrochem. Soc.* **2001**, *148*, 60−64.
(11) Gherardini, L.; Michaud, P. A.; Panizza, M.; Comninellis, C.; Vatistas, N. Electrochemical oxidation of 4-chlorophenol for wastewater treatment: Definition of normalized current efficiency (Φ). *J. Electrochem. Soc.* **2001**, *148*, 78−82.
(12) Cañizares, P.; García-Gómez, J.; Sáez, C.; Rodrigo, M. A. Electrochemical oxidation of several chlorophenols on diamond electrodes. Part I. Reaction mechanism. *J. Appl. Electrochem.* **2003**, *33*, 917−927.
(13) Cañizares, P.; García-Gómez, J.; Sáez, C.; Rodrigo, M. A. Electrochemical oxidation of several chlorophenols on diamond electrodes. Part II. Influence of waste characteristics and operating conditions. *J. Appl. Electrochem.* **2004**, *34*, 87−94.
(14) Cañizares, P.; Sáez, C.; Lobato, J.; Rodrigo, M. A. Electrochemical treatment of 4-nitrophenol-containing aqueous wastes using boron-doped diamond anodes. *Ind. Eng. Chem. Res.* **2004**, *43*, 1944−1951.
(15) Cañizares, P.; Sáez, C.; Lobato, J.; Rodrigo, M. A. Electrochemical treatment of 2,4-dinitrophenol aqueous wastes using boron-doped diamond anodes. *Electrochim. Acta* **2004**, *49*, 4641−4650.
(16) Nasr, B.; Abdellatif, G. Electrochemical oxidation of 2,4,6-trinitrophenol on boron-doped diamond anodes. *J. Electrochem. Soc.* **2005**, *152*, 113−116.
(17) Montilla, F.; Michaud, P. A.; Morallón, E.; Vázquez, J. L.; Comninellis, C. Electrochemical oxidation of benzoic acid at boron-doped diamond electrodes. *Electrochim. Acta* **2002**, *47*, 3509−3513.
(18) Mitadera, M.; Spataru, N.; Fujishima, A. Electrochemical oxidation of aniline at boron-doped diamond electrodes. *J. Appl. Electrochem.* **2004**, *34*, 249−254.
(19) Panizza, M.; Michaud, P. A.; Cerisola, G.; Comninellis, C. Anodic oxidation of 2-naphthol at boron-doped diamond electrodes. *J. Electroanal. Chem.* **2001**, *507*, 206−214.
(20) Panizza, M.; Delucchi, M.; Cerisola, G. Electrochemical degradation of anionic surfactants. *J. Appl. Electrochem.* **2005**, *35*, 357−361.
(21) Chen, X. M.; Chen, G. H.; Yue, P. L. Anodic oxidation of dyes at novel Ti/B-diamond electrodes. *Chem. Eng. Sci.* **2003**, *58*, 995−1001.
(22) Polcaro, A. M.; Mascia, M.; Palmas, S.; Vacca, A. Electrochemical degradation of diuron and dichloroaniline at a BDD electrode. *Electrochim. Acta* **2004**, *49*, 649−656.
(23) Iniesta, J.; Michaud, P. A.; Panizza, M.; Comninellis, C. Electrochemical oxidation of 3-methylpyridine at a boron-doped diamond electrode: Application to electroorganic synthesis and wastewater treatment. *Electrochem. Commun.* **2001**, *3*, 346−351.
(24) Polcaro, A. M.; Vacca, A.; Mascia, M.; Palmas, S. Oxidation at boron-doped diamond electrodes: An effective method to mineralize triazines. *Electrochim. Acta* **2005**, *50*, 1841−1847.
(25) Bellagamba, R.; Michaud, P. A.; Comninellis, C.; Vatistas, N. Electrocombustion of polyacrylates with boron-doped diamond anodes. *Electrochem. Commun.* **2002**, *4*, 171−176.
(26) Nasr, B.; Abdellatif, G.; Cañizares, P.; Sáez, C.; Lobato, J.; Rodrigo, M. A. Electrochemical oxidation of hydroquinone, resorcinol, and catechol on boron-doped diamond anodes. *Environ. Sci. Technol.* **2005**, *39*, 7234−7239.
(27) Comninellis, C. Electrocatalysis in the electrochemical conversion/combustion of organic pollutants for wastewater treatment. *Electrochim. Acta* **1994**, *39*, 1857−1962.
(28) Cañizares, P.; Lobato, J.; Paz, R.; Rodrigo, M. A.; Sáez, C. Electrochemical oxidation of phenolic wastes with boron-doped diamond anodes. *Water Res.* **2005**, *39*, 2687−2703.

Received for review April 23, 2007. Revised manuscript received July 3, 2007. Accepted July 9, 2007.

ES070955I